Master's Thesis of
Chemical and Biological Engineering

ACE2-derived peptide-based graphene field-effect transistor biosensor for the detection of SARS-CoV-2

SARS-CoV-2 감지를 위한
ACE2 유래 펩타이드 기반
그래핀 전계효과 트랜지스터 바이오센서

February 2023

Graduate School of Engineering
Seoul National University
Chemical and Biological Engineering

Soobeen Lee

ACE2-derived peptide-based graphene field-effect transistor biosensor for the detection of SARS-CoV-2

Tai Hyun Park

Submitting a master's thesis of
Chemical and Biological Engineering

February 2023

Graduate School of Engineering
Seoul National University
Chemical and Biological Engineering

Soobeen Lee

Confirming the master's thesis written by
Soobeen Lee
February 2023

Chair	Ji-Sook Hahn	(Seal)
Vice Chair	Tai Hyun Park	(Seal)
Examiner	Jihyun Kim	(Seal)

Abstract

ACE2-derived peptide-based graphene field-effect transistor biosensor for the detection of SARS-CoV-2

Soobeen Lee
School of Chemical and Biological Engineering
The Graduate School
Seoul National University

Severe acute respiratory syndrome coronavirus-2 (SARS-CoV-2) is a highly contagious coronavirus that emerged in late 2019. SARS-CoV-2 has spike (S) proteins exposed on the surface of viruses that bind to human angiotensin-converting enzyme 2 (ACE2), which plays a key role in the cell entry phase. The N-terminal hACE2 α1-helix contains most of the contacting residues in the RBD-ACE2 complex and is studied as an inhibitor for blocking the RBD-ACE2 interaction. Herein, we designed ACE2-derived peptides mimicking the binding site of ACE2 with linkers and affinity tags. The ACE2-derived peptide was overexpressed on *Escherichia coli (E. coli)*, followed by purification with nickel affinity chromatography, desalting, and size exclusion chromatography (SEC) using fast protein liquid chromatography (FPLC). Sodium dodecyl sulfate-polyacrylamide gel electrophoresis (SDS-PAGE) analysis including coomassie blue gel staining and western blot analysis demonstrated purified ACE2-derived peptides exhibited the desired size and had histidine tag. Size distribution and polydispersity index (PI) of the peptides were measured by dynamic light scattering (DLS). The function of the peptides was evaluated by performing sandwich enzyme-linked immunosorbent analysis (ELISA) with SARS-CoV-2 S protein. Peptide 1, which exhibited the highest

purity after the purification amongst the peptides was tested using further sandwich ELISA depending on its concentration and SARS-CoV-2 S protein concentration. Finally, the peptide 1 was immobilized on a graphene field-effect transistor (FET) biosensor and detected SARS-CoV-2 S protein with a limit of detection of 10 aM and 10^3 TU/ml of the PV. Hence, the ACE2-derived peptide has the potential to be used as a biomaterial of nanobiosensor for the sensitive and specific detection of SARS-CoV-2.

Keywords: SARS-CoV-2, ACE2, ACE2-derived peptide, *E. coli*, Biosensor, Graphene-FET

Student Number: 2021-26535

Table of contents

List of figures

List of abbreviations

ACE2: Angiotensin-converting enzyme 2

COVID-19: coronavirus disease

DLS: Dynamic light scattering

D.I. water: Deionized water

DMEM: Dulbecco's Modified Eagles Medium

DMSO: Dimethyl sulfoxide

E: Envelope

E. coli: Escherichia coli

EDTA: Ethylenediaminetetraacetic acid

ELISA: enzyme-linked immunosorbent analysis

FBS: Fetal bovine serum

FDA: Food and Drug Administration

FET: Field-effect transistor

FPLC: fast protein liquid chromatography

G-FET: Graphene-FET

GFP: Green fluorescent protein

HEK-293 cell: Human embryonic kidney 293 cell

IPTG: Isopropyl β-D-1-thiogalactopyranoside

LB: Lysogeny broth

LOD: Limit of detection

M: Membrane

N: Nucleocapsid

PBS: Phosphate-buffered saline

PI: Polydispersity index

PV: Pseudovirus

Pry-PEG-NTA-Ni: Pyrene-poly(ethylene glycol)-nitriloacetic acid-nickel

RBD: Receptor binding domain

RT-PCR: Reverse transcription polymerase chain reaction

SARS-CoV-2: Severe acute respiratory syndrome coronavirus-2

SDS-PAGE: Sodium dodecyl sulfate-polyacrylamide gel electrophoresis

SEC: size exclusion chromatography

S: Spike

TEV: Tobacco etch virus

Trx: Thioredoxin

TU: Transduction unit

WHO: World Health Organization

1. Introduction

Severe acute respiratory syndrome coronavirus-2 (SARS-CoV-2) induces coronavirus disease (COVID-19) and it is a highly contagious virus that incurs many confirmed cases and deaths worldwide since late 2019, threatening global public health.[1] SARS-CoV-2 is a single-stranded RNA virus comprised of structural proteins such as spike (S), envelop (E), membrane (M), and nucleocapsid (N) proteins.[2] In particular, the S protein protruding from the viral surface plays a crucial role in viral infection of the host cell, making it a target for the development of inhibitors, neutralizing antibodies, and vaccines.[3] The S protein encompasses S1 subunit and S2 subunit. Viral infection occurs when the receptor binding domain (RBD) specifically binds to the human ACE2 (hACE2) followed by the S2 subunit causing three-dimensional structural changes thus enabling the membrane fusion process.[4]

Conventional diagnosis methods for COVID-19 are molecular tests and immunoassays. Reverse transcription polymerase chain reaction (RT-PCR), which represents a molecular test, targets the SARS-CoV-2 genome by amplifying the target RNA. RT-PCR is the most widely used diagnostic method of COVID-19 worldwide and is recommended by the World Health Organization (WHO) and Food and Drug Administration (FDA). However, it takes several hours to test, requires skilled professionals, and is expensive to handle.[5] Meanwhile, immunoassays target either SARS-CoV-2 antigen or antibody produced as a result of SARS-CoV-2 infection. This assay takes about 10 to 20 minutes and is relatively inexpensive compared to other diagnostic methods. However, these methods possessed disadvantages such as the need for skilled professionals and the inappropriateness of rapid diagnosis of the infection, respectively.[6] Therefore, to overcome these overall limitations for rapid detection of SARS-CoV-2 with high sensitivity, high selectivity, low cost, portability, and convenience to use, the development of nanobiosensors is actively proceeded.[7]

The nanobiosensor platform consists of biomaterials and a signal transducer with nanomaterials. Biomaterials such as peptides, sensory receptors, and nanovesicles selectively bind to target molecules. These are immobilized onto the nanomaterials of signal transducers such as field-effect transistors (FETs) and thereby transform physical and chemical changes induced by specific interactions with target molecules to amplified electrical signals.[8] In this study, hACE2-derived peptides are used as biomaterials and

these are immobilized onto graphene-FETs (g-FETs), signal transducer using pyrene-poly(ethylene glycol)-nitriloacetic acid-nickel (pry-PEG-NTA-Ni) as an interface material.

hACE2 is an essential receptor that is highly expressed in the human upper respiratory tract and is also expressed in various extrapulmonary tissues such as the heart, kidney, endothelium, and small intestine.[9] The N-terminal hACE2 α1-helix contains most of the contacting residues in the RBD-ACE2 complex, inducing hACE2-derived peptide study as an inhibitor for blocking the RBD-ACE2 interaction.[3, 4, 10-12] Notably, SARS-CoV-2 variants bind to the hACE more strongly so that hACE2 has the potential to be used as an effective biomaterial of nanobiosensor for the diagnosis of SARS-CoV-2.[10] Meanwhile, graphene is a two-dimensional material in which carbon atoms located at the corner of a hexagonal structure are sp^2 hybridized.[13] Graphene exhibits suitable properties for application in the biosensor, including its superior mobility, good signal-to-noise ratio[14], and the possibility used for scaled devices without a short-channel effect.[15] Furthermore, graphene can easily be integrated with Si-based electronic devices, making it easy to fabricate.[16] Among various sensing mechanisms, field-effect has been exploited to design the first g-FETs and inspired considerable studies for high-performance biological sensors. The graphene channel specifically interacts with target analytes and then the changed electrical conductance of graphene indicates specific binding between them occurs.[17] Ideal graphene is highly chemically inert because its surface is free of dangling bonds.[14] Thus, the functionalization is achieved using both covalently and non-covalently.[18] Non-covalent functionalization is preferable since it enables the introduction of a functional group capable of binding to a target analyte and maintains the electrical properties of graphene without modifying the structure of graphene at the same time.[19] Pyr-PEG-NTA is a bifunctional compound that is utilized as an interface material for the non-covalent functionalization of the His-tagged biomaterials with orientation. Pyrene π-π stacking onto the graphene channel and PEG reduces the surface density of tris-NTA, interacting with His-tagged ACE2-derived peptide after nickel-NTA chelation.[20]

2. Materials and methods

2.1. Gene cloning

2.1.1. Gene design of ACE2-derived peptide

ACE2-derived peptides were designed in the following order. (1) A carrier protein, thioredoxin, was introduced to enhance the solubility of expressed proteins on bacterial cells.[21, 22] (2) Tobacco etch virus (TEV) site was introduced next to Trx to remove Trx after protein expression in *E. coli*. (3) Binding site was derived from the α1 domain of ACE2 and can be bound to SARS-CoV-2 spike protein through its receptor-binding domain (RBD). The longest sequence of the binding sites was STIEEQAKTFLDKFNHEAEDLFYQSSL and is located 19-45 of the ACE2.[11] The others were truncated from the sequence of the longest and their inhibitory ability was confirmed with pseudotyped SARS-CoV-2 lentivirus.[12] (4) Combination of flexible (GGGGS) and rigid $(AP)_7$ linkers was designated for flexibility to reduce steric hindrance between interacting molecules and give height from the bottom for further immobilization, respectively.[23-25] 6X His affinity tag (histidine tag) is additionally introduced between Trx and arginine (Arg) tag. Schematic representation of designed ACE2-derived peptides were represented in Figure 2.1.

1) Carrier protein

Trx sequence

: MSDKIIHLTDDSFDTD
VLKADGAILVDFWAE
WCGPCKMIAPILDEIA
DEYQGKLTVAKLNID
QNPGTAPKYGIRGIPT
LLLFKNGEVAATKVG
ALSKGQLKEFLDANLA

2) TEV site

TEV site sequence: ENLYFQS

3) ACE2-derived peptide

① Binding sites

Amino acid sequence
STIEEQAKTFLDKFNHEAEDLFYQSSL
TFLDKFNHEAEDLFYQ
EDLFYQ

② Linkers

Characteristics	Amino acid sequence	Purpose
Flexible	GGGGS	Avoiding steric hindrance
Rigid	$(AP)_7$	Spacial separation

Linker sequence: GGGGSAPAPAPAPAPAPAPGGGGS

③ Affinity & immobilization tags

Histidine tag (HHHHHH) is utilized for further immobilization purpose of produced peptides.

Figure 2.1. Schematic representation of designed ACE2-derived peptide.

2.1.2. Gene cloning of ACE2-derived peptide

Codon-optimized sequences of ACE2-based peptides are cloned into a pET-21a(+) cloning vector which has a 6X His affinity tag at the C-terminus for the further purification step. Gene synthesis procedures were conducted by BIONICS Co., Ltd.

2.2. Production

Figure 2.2 represents a schematic illustration of the overall ACE2-derived peptide production steps.

2.2.1. Expression of ACE2-derived peptide in *E. coli*

All kinds of ACE2-derived peptides were expressed in the following manner. The pET-21a(+) ACE2-derived proteins constructs were transformed to a Rosetta (DE3) and incubated in 100 μg/mL ampicillin argar plates for 16 h at 37℃. A single colony was inoculated into a 5 mL lysogeny broth (LB) medium with 100 μg/mL ampicillin and incubated for 16 h at 37℃. 1 mL of the cultured cell was added into 200 mL LB medium with 100 ug/mL ampicillin and then incubated for 16 h at 37℃. The cells were added into 6 flasks of 1 L LB medium, respectively, and then incubated at 37℃ until the optical density (OD600) value reached 0.5~0.6. Isopropyl β-D-1-thiogalactopyranoside (IPTG) is added to induce overexpression of the ACE2-derived proteins to a final concentration of 1 mM and then incubated for 4 h at 37℃. The cells were harvested using a centrifuge (7,000 × g, 10 min, 4℃) and pellets were separated.

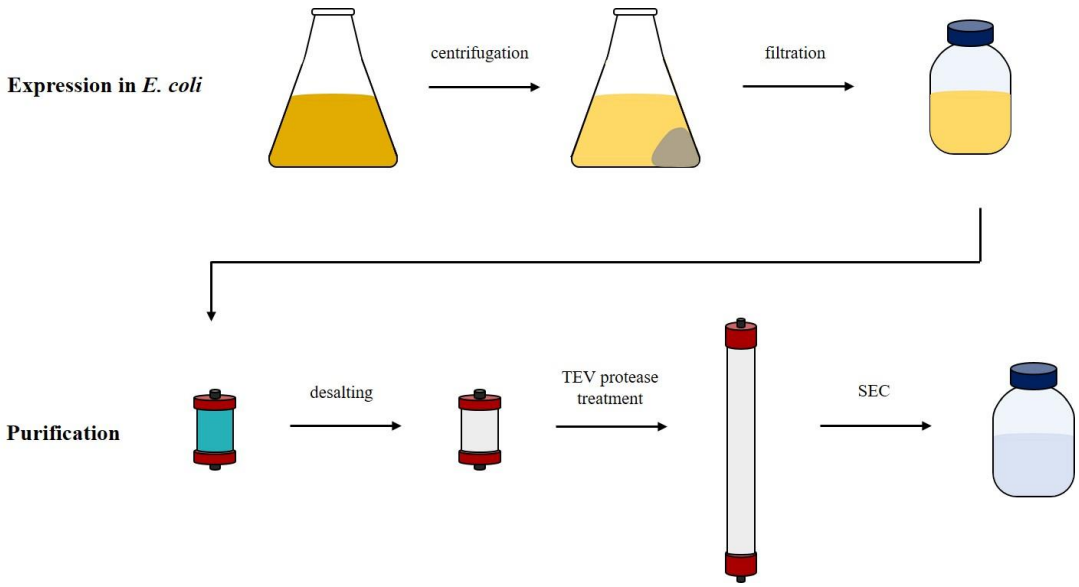

Figure 2.2. Illustration of the overall ACE2-derived peptide production steps.

2.2.2. Purification of ACE2-derived peptide in *E. coli*

2.2.2.1. Nickel affinity chromatography

The separated pellets were suspended in binding buffer (20 mM Tris-HCl, 0.5 M NaCl, 20 mM imidazole, pH 8.0). The suspended cells were lysed by sonication (5 s on/off, 30% amplitude, 5 min) and centrifuged (12,000 × g, 30 min, 4℃). The supernatant containing the ACE2-derived proteins is filtered by a 0.45 μm bottle top filter. Meanwhile, fast protein liquid chromatography (FPLC) (GE Healthcare) was equipped with HisTrap HP column (Cytiva) and the filtered supernatant was loaded to the column equilibrated with binding buffer. Next, the column was gradually washed by washing buffer (20 mM Tris-HCl, 0.5 M NaCl, 50 mM imidazole, pH 8.0). The ACE2-derived proteins were eluted after elution buffer (20 mM Tris-HCl, 0.5 M NaCl, 350 mM imidazole, pH 8.0) were treated.

2.2.2.2. Desalting

The purified ACE2-derived peptides were desalted by exchanging elution buffer for HEPES buffer II (20 mM HEPES-NaOH, 100 mM, pH 8.0) using HiTrap HP desalting column (Cytiva).

2.2.2.3. Size exclusion chromatography

To eliminate carrier protein, TEV protease at a molar ratio of 1:100 was incubated with the desalted ACE2-derived peptide for 4 h 37℃. Meanwhile, size exclusion chromatography (SEC) (Cytiva) using column (Superdex 200 Increase 10/300 GS, Cytiva) and 2 mL was equilibrated with HEPES buffer II. The mixture was injected through the loop to separate the small size of ACE2-derived peptides from the larger size of carrier protein and TEV protease. Finally, the absorbance of purified ACE2-derived peptides was measured at 280 nm using a Microplate reader (TECAN) and then the absorbance values were converted to concentrations.

2.3. Characterization

2.3.1. SDS-PAGE

2.3.1.1. Coomassie blue gel staining

Coomassie blue gel staining and western blot analysis were executed to determine the size of the purified ACE2-derived peptides and the size of confirmed peptides including his tag, respectively. Sodium dodecyl-sulfate polyacrylamide gel electrophoresis (SDS-PAGE) was polyacrylamide gel and samples were prepared. Polyacrylamide gel with 20 % acrylamide which can resolve protein size of at least 4 kDa was used. Samples collected at each step of peptide purification were loaded to each well and protein marker PM2700 (SMOBIO) was loaded. SDS-PAGE was performed at 80 V. Coomassie blue gel staining was conducted by incubating the gel with coomassie blue staining solution [0.5 g/L coomassie blue, 7% (v/v) acetic acid, 40% (v/v) methanol] for 1 h at room temperature. The stained gel was incubated with destaining solution I [7% (v/v) acetic acid, 40% (v/v) methanol] for 1 h at room temperature and followed by incubating with destaining solution II [7% (v/v) acetic acid, 5% (v/v) methanol] for 16 h at room temperature.

2.3.1.2. Western blot

The SDS-PAGE gels were transferred to a nitrocellulose membrane, incubating with a blocking solution [5 wt % skim milk in PBS-T (1X PBS, 0.1 vol % Tween-20)] for 1 h at room temperature. A his-probe mouse monoclonal IgG was used as a primary antibody, and a goat anti-mouse IgG-HRP (Ab frontier) was used as a secondary antibody. And washing with 0.1% PBS-T was conducted at every step. Finally, detection of the ACE2-derived peptides was conducted by treating TOPview ECL Pico Plus Western Substrate (Enzynomcis).

2.3.2. DLS measurement

The size distribution and homogeneity of ACE2-derived peptides were analyzed by a DLS spectrophotometer (DLS-7000). The measurement was conducted five times at room temperature and averaged values were utilized.

2.3.3. Sandwich ELISA with SARS-CoV-2 S protein

We conducted three types of sandwich ELISA to validate the functionality of produced ACE2-derived peptides and a schematic representation of the experimental steps is illustrated in Figure 2.3. All sorts of ACE2-derived peptides were bound to SARS-CoV-2 spike S1-biotin to pick up one kind of ACE2-derived peptide and conduct further assays (Fig.). All experimental steps were performed in the same manner regarding all sorts of ACE2-derived peptides. 100 μL of ACE2-derived peptide (50 μM in HEPES buffer II) was added to six wells of a nickel-coated 96-well white plate (Thermo Scientific) and incubated for 1 h at room temperature. Blocking was conducted with 100 μL of 1X Blocking Buffer 2 for 30 min at room temperature. 40 μL of SARS-CoV-2 spike S1-biotin (50 nM in 1X Immuno Buffer 1) and 40 μL of 1X Immuno Buffer 1 were applied in three wells, respectively, and then incubated for 1 h at room temperature. Blocking was conducted in the same manner as described above. 100 μL of Sterptavidin-HRP (1:1,000 in 1X Blocking Buffer 2) was treated to each well and incubated for 1 h at room temperature. Again, blocking was conducted in the same manner as described above. A mixture of ELISA ECL Substrate A and ELISA ECL Substrate B [50% (v/v)] was added to each well and read chemiluminescence immediately using a Microplate reader (TECAN). Washing was conducted between every step and with 150 μL of 1X Immuno Buffer 1 three times.

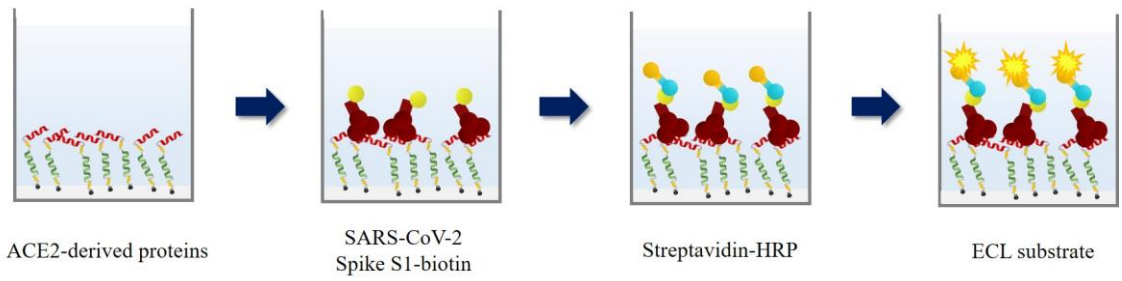

Figure 2.3. Schematic diagram of sandwich ELISA experimental steps.

2.4. Production of SARS-CoV-2 PV

Human embryonic kidney (HEK) 293T cells were incubated in Dulbecco's Modified Eagles Medium (DMEM) [(10% fetal bovine serum (FBS)] and transferred to a 100 pi dish. The cells were incubated overnight at 37℃ in an incubator conditioned with 5% CO_2 until the cell density reaches 70-90% confluence.[26] 12 μg of DNA combination of pBoB-SARS-CoV-2 spike, pLP1, pLP2, and pLVXS-IRES-zsgreen1 was transfected with Lipofectamine 3000 (Invitrogen). The transfected cells were incubated for 48 h at 37℃ in an incubator conditioned with 5% CO_2. SARS-CoV-2 PV with S protein-containing supernatant was harvested by centrifugation (1,000 g, 10 min, 25℃) and then concentrated using Amicon Ultra-15 centrifugal filters (Millipore). The produced SARS-CoV-2 PV with S protein was titrated using One Wash Lentivirus Titer Kit HIV-1 p24 ELISA (Origene)[27] and its concentration was 3.7×10^{7} Transduction unit (TU)/mL. Aliquots of the SARS-CoV-2 PV with S protein were stored at -80℃.

2.5. Preparation of ACE2-derived peptide on g-FET

A mixture of 2 mM pry-PEG-NTA in Dimethyl sulfoxide (DMSO) (NANOSC) and 100 mM $NiSO_4\cdot H_2O$ in Deionized water (D.I. water) (Sigma-Aldrich) [50% (v/v)) was incubated for 1 h at room temperature, then 2 μL of the mixture was dropped onto the graphene of g-FET and incubated for 1 h at room temperature. After rinsing three times with 0.1X PBS, 2 μL of 100 nM ACE2-derived peptide 1 was applied onto the graphene and then incubated for 3 h at room temperature. After washing in the same manner, the ACE2-derived peptide 1-based g-FET was rinsed with D.I. water and dried at room temperature. Electrical characteristics are measured by 2636A System SourceMeter (Keithley) and probe station MST8000C (MSTECH). First, we carried out the current-voltage curves over a range from -1.0 to +1.0 V of the bare graphene, pyr-Ni, and peptide 1 immobilized on g-FET, respectively. Next, output curves of the peptide 1-based g-FET with various gate voltages from 0 V to -1.5 V in steps of -0.3 V.

Electrical characteristics are measured by 2636A System SourceMeter (Keithley) and probe station MST8000C (MSTECH). The electrical signal was normalized as $[\Delta I/I_0] = (I-I_0)/I_0$, where I is the real-time current and I_0 is the initial current.[17, 28]

3. Results and discussion

3.1. Production of ACE2-derived peptide

ACE2-derived peptide overexpressed in *E. coli* was purified with nickel affinity column equipped FPLC, which selectively remains histidine-containing proteins. Second, desalting was performed to remove imidazole. Third, TEV protease was treated to eliminate unwanted Trx carrier protein after ACE2-derived peptides were expressed in *E .coli*. Finally, SEC was conducted. SEC chromatogram of ACE2-derived peptides was represented in Figure 3.1 and they exhibited similar tendencies. Four significant peaks were observed and solutions corresponding to the peaks were eluted individually. We expected that the fourth eluent (E4) contain ACE2-derived peptides since the SEC separates proteins as their size and smaller proteins eluted later.

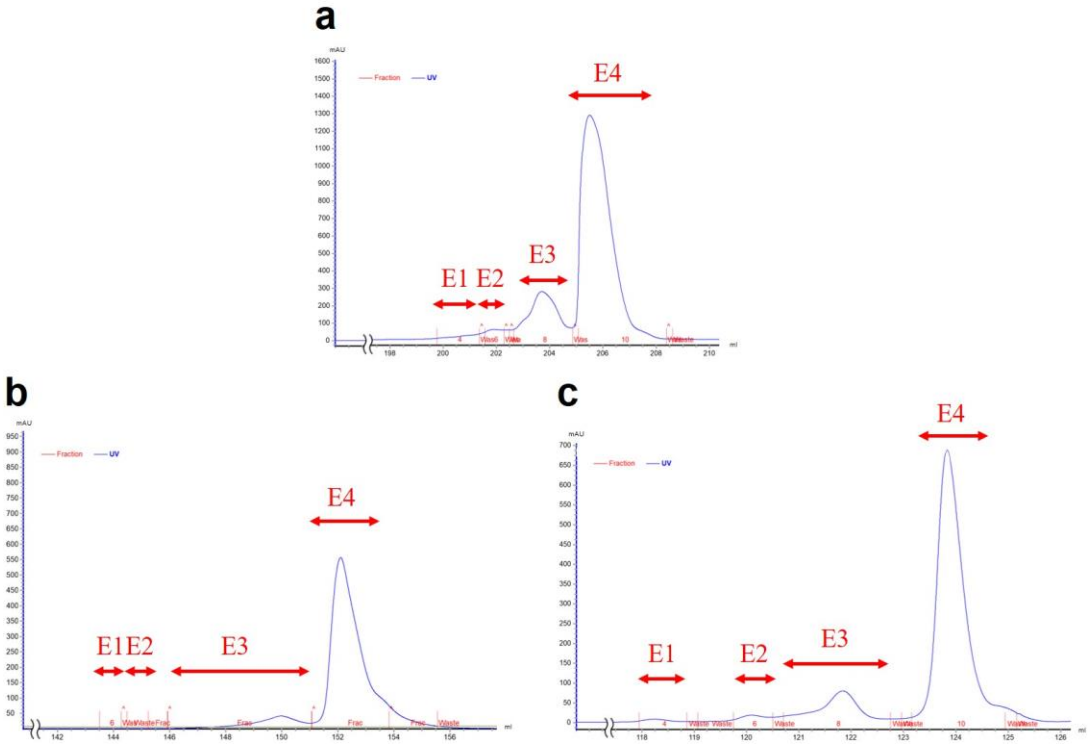

Figure 3.1. Representative chromatograms of SEC curves. (a) SEC chromatogram of peptide 1 (b) SEC chromatogram of peptide 2 (c) SEC chromatogram of peptide 3.

3.2. Characterization of ACE2-derived peptide

3.2.1. SDS-PAGE

SEC eluents and samples collected before SEC chromatography were analyzed by SDS-PAGE. As we expected, E4 lanes contained desired ACE2-derived peptides (red arrows). Coomassie blue gel staining confirmed the size of ACE2-derived peptide 1, peptide 2, and peptide 3 of 7, 6, and 4 kDa, respectively. (Figure 3.2a, Figure 3.3a, and Figure 3.4a) Furthermore, western blot analysis using histidine antibody verified the desired peptide has a histidine tag. (Figure 3.2b, Figure 3.3b, and Figure 3.4b)

3.2.2. DLS measurement

The size of ACE2-derived peptides was analyzed using DLS and their sizes were within 10 nm. (Figure 3.5a) Peptide 1 exhibited a single peak, unlike other peptides. PI of all peptides was measured and confirmed peptide 1 was purified with the highest purity.

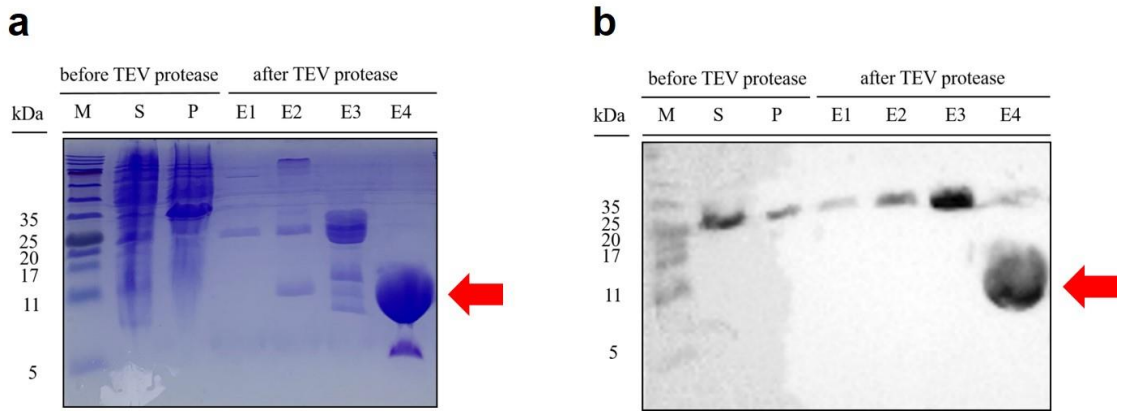

Figure 3.2. SDS-PAGE results of peptide 1. (a) Coomassie blue gel staining of peptide 1 (b) Western blot of peptide 1.

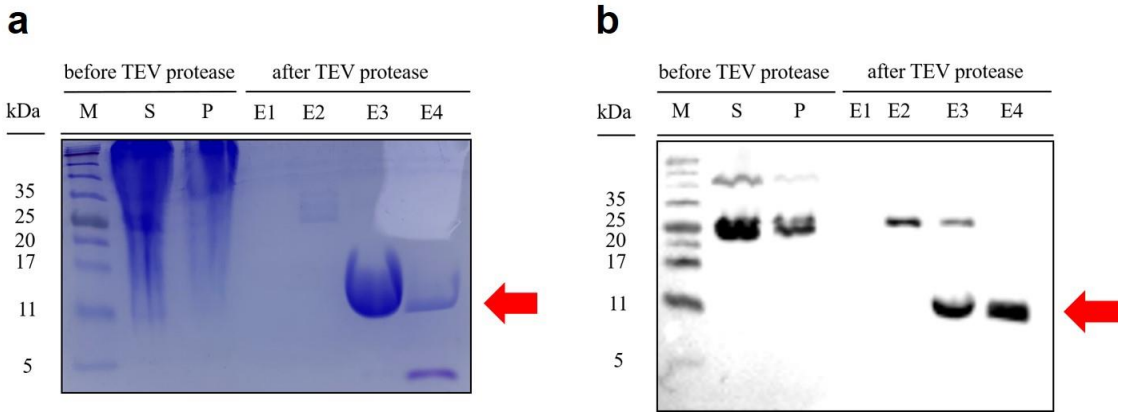

Figure 3.3. SDS-PAGE results of peptide 2. (a) Coomassie blue gel staining of peptide 2 (b) Western blot of peptide 2.

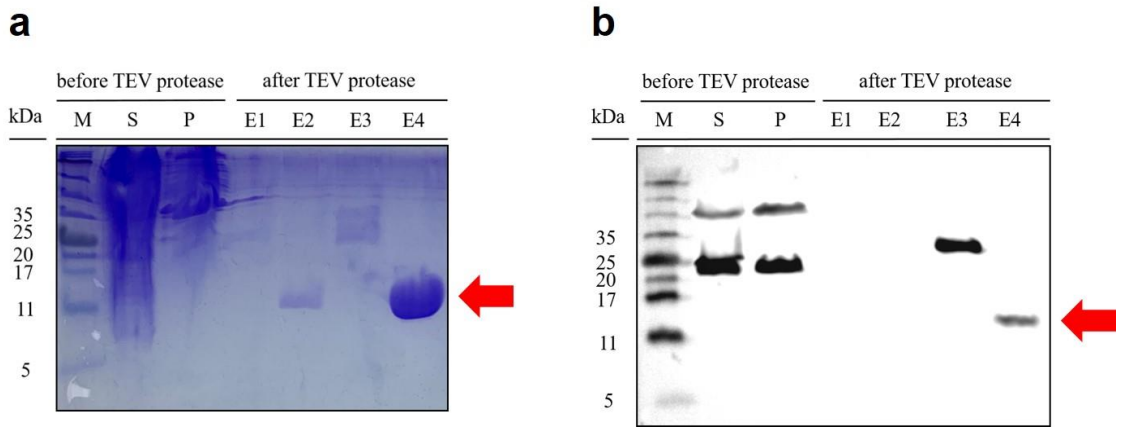

Figure 3.4. SDS-PAGE results of peptide 3. (a) Coomassie blue gel staining of peptide 3 (b) Western blot of peptide 3.

a

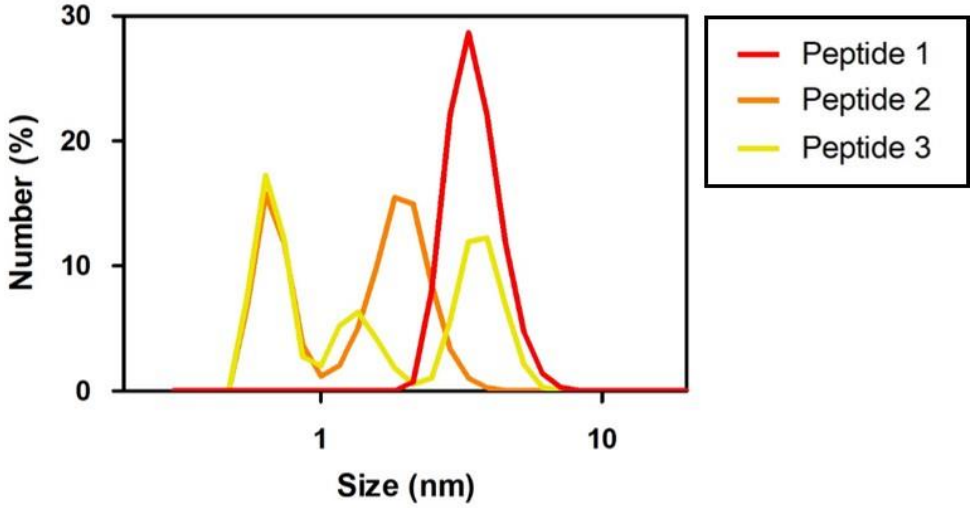

b

Name	Amino acid sequence of binding site	PI
Peptide 1	STIEEQAKTFLDKFNHEAEDLFYQSSL	0.4
Peptide 2	TFLDKFNHEAEDLFYQ	0.7
Peptide 3	EDLFYQ	0.6

Figure 3.5. DLS results of ACE2-derived peptides. (a) Size distribution of ACE2-derived peptides (b) PI of ACE2-derived peptides.

3.2.3. Sandwich ELISA with SARS-CoV-2 S protein

The binding of peptide 1 and SARS-CoV-2 spike S1-biotin was demonstrated with varying concentrations of SARS-CoV-2 spike S1-biotin of 2-fold dilution. 100 μL of peptide 1 (0.1 μM in HEPES buffer II) was added to thirty wells of the nickel-coated 96-well white plate (Thermo Scientific) and incubated for 1 h at room temperature. Blocking was conducted with 100 μL of 1X Blocking Buffer 2 for 30 min at room temperature. 40 μL of SARS-CoV-2 spike S1-biotin (2-fold dilution from 1024 nM to 2 nM in 1X Immuno Buffer 1) was added to each of the three wells. The following steps were conducted in the same manner described in 2.3.3.. Furthermore, specificity tests were conducted with varying concentrations of concentration of peptide 1 to verify the amount of peptide 1 affects the binding capacity of SARS-CoV-2 spike S1-biotin. 100 μL of peptide 1 (0.4 μM, 2 μM, 10 μM in HEPES buffer II) was added to each of six wells of the nickel-coated 96-well white plate (Thermo Scientific) and incubated for 1 h at room temperature. Blocking was conducted with 100 μL of 1X Blocking Buffer 2 for 30 min at room temperature. 40 μL of SARS-CoV-2 spike S1-biotin (50 nM in 1X Immuno Buffer 1) and 40 μL of 1X Immuno Buffer 1 were applied in three wells, respectively, and then incubated for 1 h at room temperature. The following steps were conducted in the same manner described above. The results of sandwich ELISA confirmed the interaction SARS-CoV-2 S protein bind to the ACE2-derived peptide by the relative light unit (RLU) signals amplified by the biotin-streptavidin system. First, the binding ability of the purified ACE2-derived peptides was tested and they exhibited no statistical significance. (Figure 3.6) However, considering the previous UV value of the SEC chromatogram and the DLS results, peptide 1 was used in further characterizations. We investigated the signal response in a dose-dependent manner (Figure 3.7a). Besides, a specificity test was conducted whether the previous dose-dependent signals were attributed to the S protein bound to the nickel-coated plate non-specifically. (Figure 3.7b) Notably, the signal was also dependent on the concentration of peptide 1, clarifying the interaction between the two was found to be specific binding.

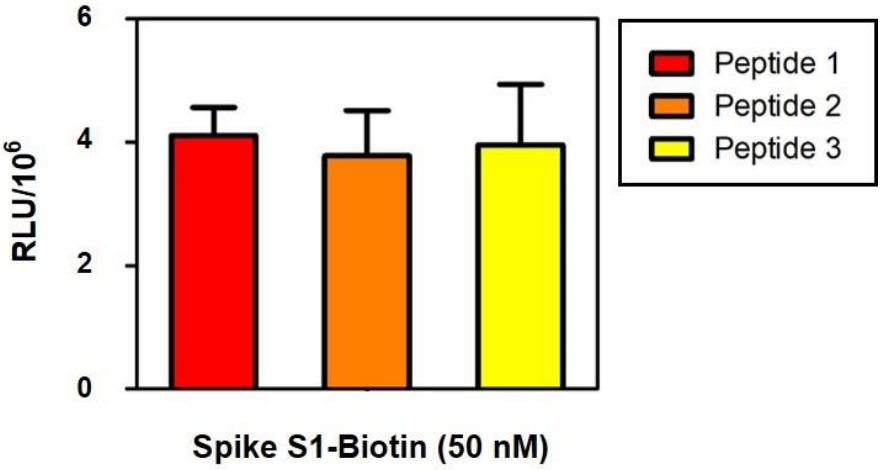

Figure 3.6. Sandwich ELISA results of ACE2-derived peptides upon SARS-CoV-2 S protein to compare their binding ability.

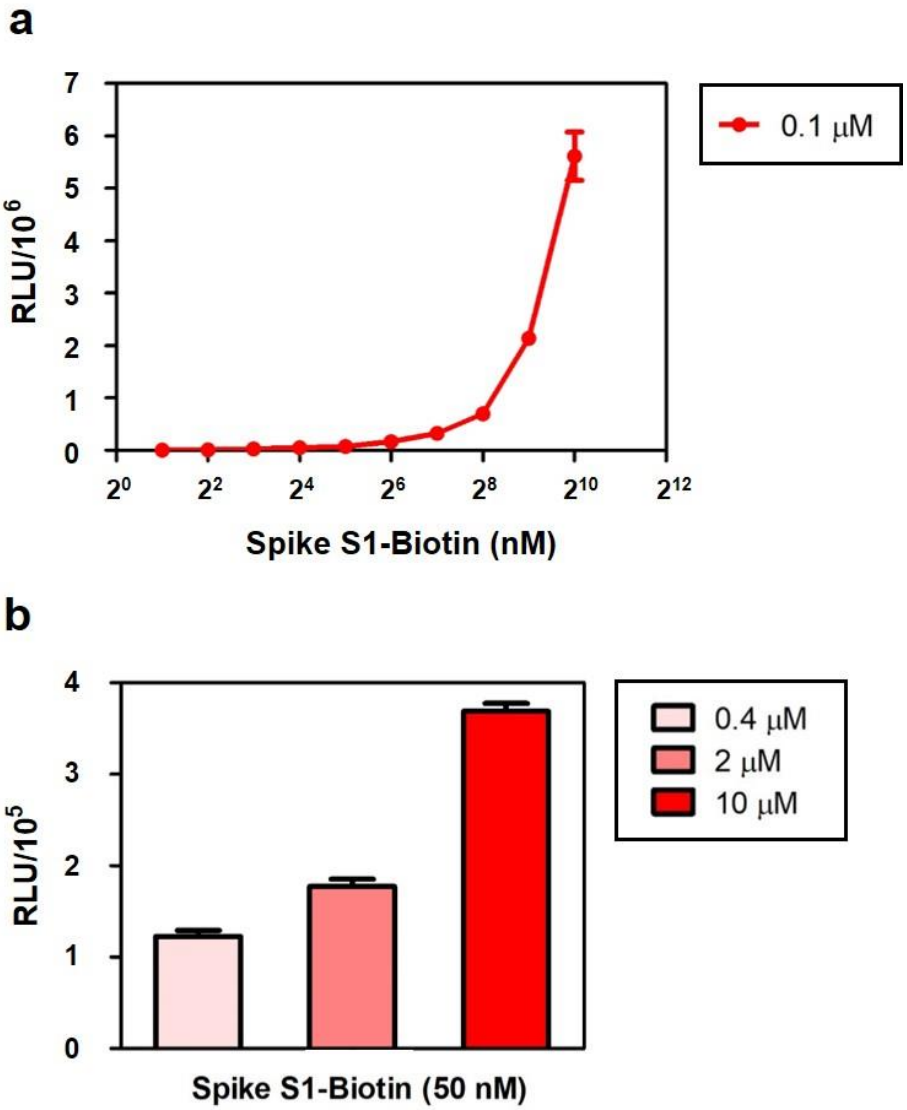

Figure 3.7. Sandwich ELISA results of peptide 1 upon SARS-CoV-2 S protein. (a) Dose-dependent curve of peptide 1 (b) Specificity test of peptide 1.

3.3. Application of ACE2-derived peptide

3.3.1. Production of SARS-CoV-2 PV

The green fluorescent protein (GFP) expressing cells were observed using a fluorescence microscope at 20× to examine transfection in HEK293T cells.[27] (Figure 3.8)

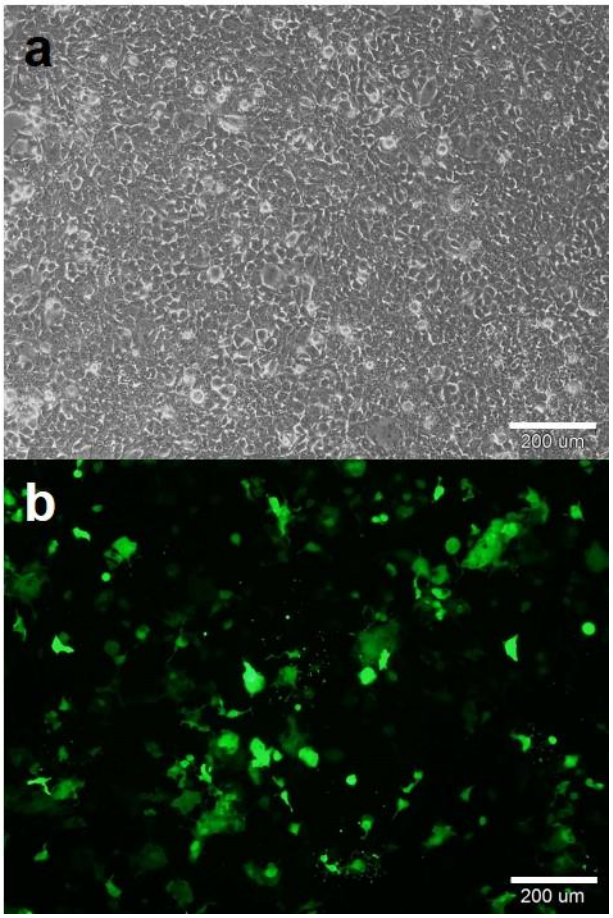

Figure 3.8. Microscopic images of GFP expression in HEK293T cells at 48 h post-transduction with lentiviral vectors. (a) Bright-field images of HEK293T cells (b) Green fluorescence images of HEK293T cells.

3.3.2. Immobilization of ACE2-derived peptide on g-FET

A schematic representation of peptide 1-based g-FET is illustrated in Figure 3.9a. Figure 3.9b shows the current-voltage curves. Peptide 1 immobilized g-FET exhibits reliable electrical contacts since the I-V relationship is linear.[28] The effect of positive gate voltage reduces the current of the p-type g-FET as shown in Figure 3.9c.

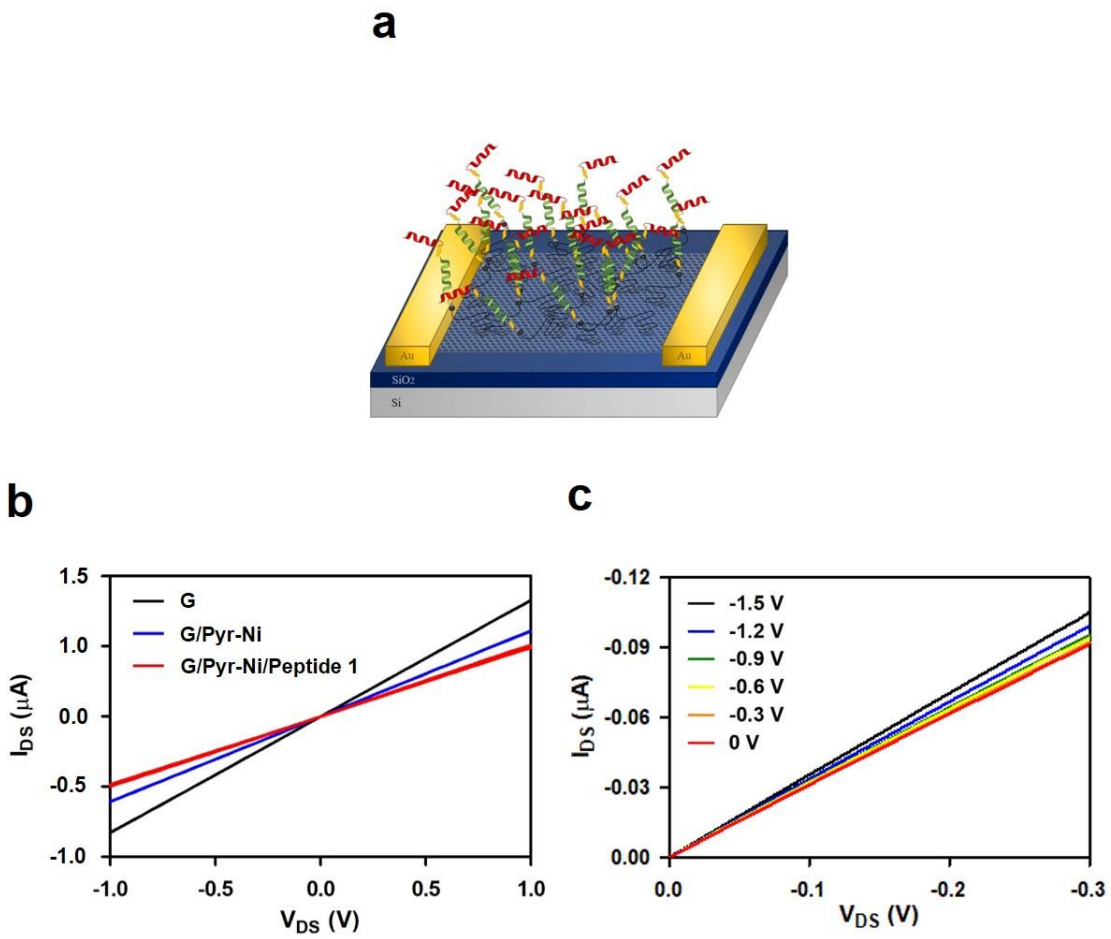

Figure 3.9. Electrical characterization of pristine, pry-PEG-NTA-Ni modified, and peptide 1 immobilized g-FET. (a) Schematic illustration of peptide 1-based g-FET (b) Current-voltage curves of peptide 1-based g-FET (c) Output curves of peptide 1-based g-FET.

3.3.3. Real-time sensing with SARS-CoV-2 S protein

Figure 3.10a shows the real-time response of the ACE2-derived peptide 1-based g-FET sensor upon SARS-CoV-2 S protein. When 0.1X PBS is applied to a graphene channel, the current recovery to the base current. In contrast, when specific binding of S protein to peptide 1 occurs, positively charged S protein diluent at pH 7 induced negatively increased current since major carriers (holes) in the graphene channel decreased.[14] Meanwhile, there is no significant signal from the pristine g-FET. Surprisingly, the fabricated biosensor detected a limit of detection (LOD) of 10 aM of S protein, which represents the highly sensitive performance of the device. Furthermore, the result of normalized dose-dependent response curves from 10^{0} to 10^{-6} M suggests that the fabricated biosensor has the potential to be applied for COVID-19 diagnosis.[17] Figure 3.10b represents the normalized response negatively increased as the S protein dose increased.

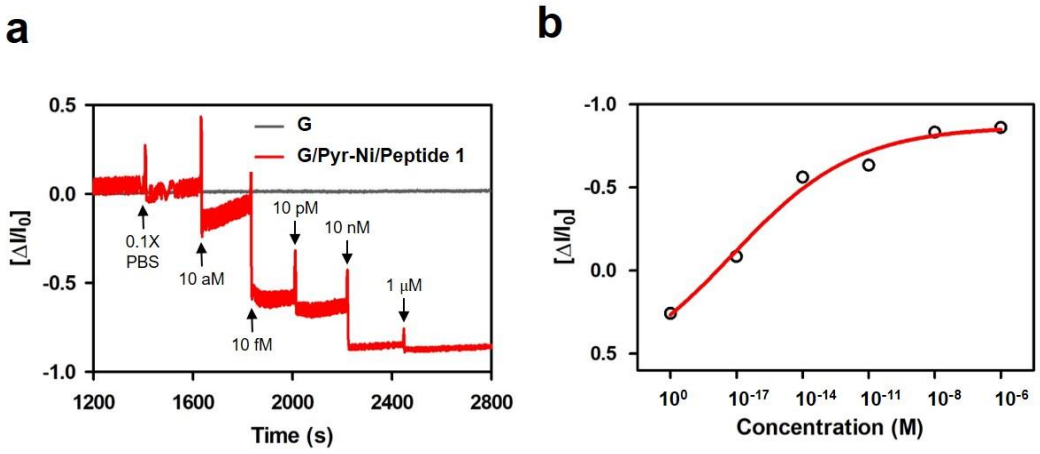

Figure 3.10. Detection of SARS-CoV-2 S protein. (a) Real-time sensing curves of peptide 1-based g-FET (b) Related dose-dependent response curve.

3.3.4. Real-time sensing with SARS-CoV-2 PV

Figure 3.11 shows the real-time response of the ACE2-derived peptide 1-based g-FET sensor upon SARS-CoV-2 PV with S protein. The binding of negatively charged PV diluents at pH 7 to peptide 1 produced a positively increased current since major carriers (holes) in the graphene channel increased.[14]

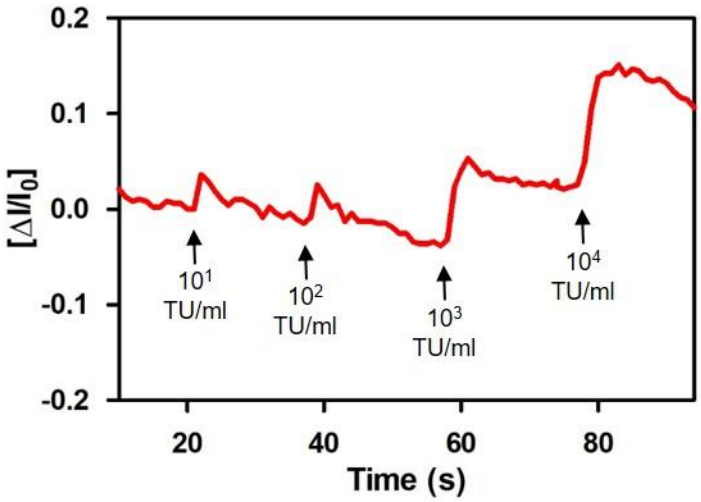

Figure 3.11. Real-time sensing curves of peptide 1-based g-FET upon SARS-CoV-2 PV.

4. Conclusion

Since the advent of the SARS-CoV-2, rapid and sensitive diagnosis of COVID-19 has been required. ACE2 is an essential receptor for the SARS-CoV-2 viral infection and some part of its amino acid sequences has been utilized in the form of the peptide to inhibit the interaction between the ACE2 and the virus. Implementing ACE2-derived peptides has the potential for the specific binding of the SARS-CoV-2 and holds possibilities for even more robust detection methods for the variants. We produced an ACE2-derived peptide in *E. coli* and it is immobilized on g-FET for the detection of SARS-CoV-2. The fabricated biosensor was able to detect SARS-CoV-2 S protein in a dose-dependent manner with a LOD of 10 aM, which represents this biosensor is highly responsive. Furthermore, the sensor detected PV, mimicking more real shapes of the SARS-CoV-2. Therefore, the purified ACE2-derived peptide has the potential to be used as a biomaterial constituting a nanobiosensor for the detection of SARS-CoV-2.

Bibliography

1. Smyrlaki I, Ekman M, Lentini A, Rufino de Sousa N, Papanicolaou N, Vondracek M, et al. Massive and rapid COVID-19 testing is feasible by extraction-free SARS-CoV-2 RT-PCR. Nat Commun. 2020;11(1):4812.
2. Yang H, Rao Z. Structural biology of SARS-CoV-2 and implications for therapeutic development. Nat Rev Microbiol. 2021;19(11):685-700.
3. Schutz D, Ruiz-Blanco YB, Munch J, Kirchhoff F, Sanchez-Garcia E, Muller JA. Peptide and peptide-based inhibitors of SARS-CoV-2 entry. Adv Drug Deliv Rev. 2020;167:47-65.
4. Yang J, Petitjean SJL, Koehler M, Zhang Q, Dumitru AC, Chen W, et al. Molecular interaction and inhibition of SARS-CoV-2 binding to the ACE2 receptor. Nat Commun. 2020;11(1):4541.
5. Zhou Y, Zhang L, Xie YH, Wu J. Advancements in detection of SARS-CoV-2 infection for confronting COVID-19 pandemics. Lab Invest. 2022;102(1):4-13.
6. Taleghani N, Taghipour F. Diagnosis of COVID-19 for controlling the pandemic: A review of the state-of-the-art. Biosens Bioelectron. 2021;174:112830.
7. Kevadiya BD, Machhi J, Herskovitz J, Oleynikov MD, Blomberg WR, Bajwa N, et al. Diagnostics for SARS-CoV-2 infections. Nat Mater. 2021;20(5):593-605.
8. Moon D, Cha YK, Kim SO, Cho S, Ko HJ, Park TH. FET-based nanobiosensors for the detection of smell and taste. Sci China Life Sci. 2020;63(8):1159-67.
9. Huang Y, Yang C, Xu XF, Xu W, Liu SW. Structural and functional properties of SARS-CoV-2 spike protein: potential antivirus drug development for COVID-19. Acta Pharmacol Sin. 2020;41(9):1141-9.
10. Han P, Su C, Zhang Y, Bai C, Zheng A, Qiao C, et al. Molecular insights into receptor binding of recent emerging SARS-CoV-2 variants. Nat Commun. 2021;12(1):6103.
11. Kuznetsov A, Järv J. Mapping of ACE2 binding site on SARS-CoV-2 spike protein S1: docking study with peptides. Proceedings of the Estonian Academy of Sciences. 2020;69(3).
12. Larue RC, Xing E, Kenney AD, Zhang Y, Tuazon JA, Li J, et al. Rationally Designed ACE2-Derived Peptides Inhibit SARS-CoV-2. Bioconjug Chem. 2021;32(1):215-23.

13. Lui CH, Liu L, Mak KF, Flynn GW, Heinz TF. Ultraflat graphene. Nature. 2009;462(7271):339-41.
14. Fu W, Jiang L, van Geest EP, Lima LM, Schneider GF. Sensing at the Surface of Graphene Field-Effect Transistors. Adv Mater. 2017;29(6).
15. Hess LH, Seifert M, Garrido JA. Graphene Transistors for Bioelectronics. Proceedings of the IEEE. 2013;101(7):1780-92.
16. Yang G, Lee C, Kim J, Ren F, Pearton SJ. Flexible graphene-based chemical sensors on paper substrates. Phys Chem Chem Phys. 2013;15(6):1798-801.
17. Seo G, Lee G, Kim MJ, Baek SH, Choi M, Ku KB, et al. Rapid Detection of COVID-19 Causative Virus (SARS-CoV-2) in Human Nasopharyngeal Swab Specimens Using Field-Effect Transistor-Based Biosensor. ACS Nano. 2020;14(4):5135-42.
18. Tran T-T, Mulchandani A. Carbon nanotubes and graphene nano field-effect transistor-based biosensors. TrAC Trends in Analytical Chemistry. 2016;79:222-32.
19. Georgakilas V, Tiwari JN, Kemp KC, Perman JA, Bourlinos AB, Kim KS, et al. Noncovalent Functionalization of Graphene and Graphene Oxide for Energy Materials, Biosensing, Catalytic, and Biomedical Applications. Chem Rev. 2016;116(9):5464-519.
20. Jorde L, Li Z, Pöppelwerth A, Piehler J, You C, Meyer C. Biofunctionalization of carbon nanotubes for reversible site-specific protein immobilization. Journal of Applied Physics. 2021;129(9).
21. LaVallie ER, DiBlasio EA, Kovacic S, Grant KL, Schendel PF, McCoy JM. A thioredoxin gene fusion expression system that circumvents inclusion body formation in the E. coli cytoplasm. Biotechnology (N Y). 1993;11(2):187-93.
22. Paraskevopoulou V, Falcone FH. Polyionic Tags as Enhancers of Protein Solubility in Recombinant Protein Expression. Microorganisms. 2018;6(2).
23. Chen X, Zaro JL, Shen WC. Fusion protein linkers: property, design and functionality. Adv Drug Deliv Rev. 2013;65(10):1357-69.
24. Li G, Huang Z, Zhang C, Dong BJ, Guo RH, Yue HW, et al. Construction of a linker library with widely controllable flexibility for fusion protein design. Appl Microbiol Biotechnol. 2016;100(1):215-25.
25. Klein JS, Jiang S, Galimidi RP, Keeffe JR, Bjorkman PJ. Design and characterization of structured protein linkers with differing flexibilities. Protein Eng Des Sel. 2014;27(10):325-30.
26. Li Q, Wu J, Nie J, Zhang L, Hao H, Liu S, et al. The Impact of Mutations in SARS-CoV-2 Spike on Viral Infectivity and Antigenicity. Cell. 2020;182(5):1284-94 e9.
27. Kalidasan V, Ng WH, Ishola OA, Ravichantar N, Tan JJ, Das KT. A guide in

lentiviral vector production for hard-to-transfect cells, using cardiac-derived c-kit expressing cells as a model system. Sci Rep. 2021;11(1):19265.

28. Ahn SR, An JH, Lee SH, Song HS, Jang J, Park TH. Peptide hormone sensors using human hormone receptor-carrying nanovesicles and graphene FETs. Sci Rep. 2020;10(1):388.

Abstract in Korean

중증급성호흡기증후군 코로나바이러스-2(SARS-CoV-2는 2019년 후반에 등장하였고 전염성과 감염성이 높은 코로나바이러스이다. SARS-CoV-2는 인간 안지오텐신전환 효소2 (hACE2)에 결합하는 스파이크 (S) 단백질이 표면에 노출되어 있으며, 이것은 세포 내 이입에 핵심적인 역할을 한다. N-터미널의 hACE2의 α1-helix 펩타이드는 S 단백질의 수용체 결합 도메인 (RBD)과 결합하는 부위로서 RBD-ACE2 상호작용을 차단하기 위한 차단제로서 연구되어오고 있다.

한편 현재까지 주로 사용되는 코로나바이러스의 진단 방식은 역전사 중합 효소 연쇄반응 (RT-PCR)과 측면 유동 검사 (LFA)이다. 먼저 RT-PCR의 경우 WHO와 FDA의 승인을 받은 가장 많이 사용되고 있는 진단법으로, 높은 정확도를 갖지만 진단까지 최소 6시간이 소요되고 전문 인력이 필요하다는 특징을 갖는다. LFA의 경우에는 사용이 간편하고 진단까지 10분 정도가 소요되지만, 검출하기 위해 상대적으로 많은 양의 검체가 필요한 실정이다.

본 논문에서는 신속하면서도 민감한 코로나바이러스 진단을 위한 나노바이오센서를 개발하는 것을 목표로 한다. 먼저 센서에 적용되기 용이한 형태의 재조합 ACE2 유래 펩타이드를 대장균에서 과발현시킨 후 세 가지 단계를 거쳐 정제하였다. 니켈 친화성, 탈염, 크기 배제 컬럼을 장착한 고속 단백질 액체 크로마토그래피 (FPLC)를 사용하여 진행하였다. 정제된 ACE2 유래 펩타이드는 단백질 전기영동 (SDS-PAGE)을 통해 원하는 크기와 어피니티 태그를 포함하는 것을 확인하였다. 이후 동적 광산란 (DLS) 측정을 통해 정제 산물 내 펩타이드의 사이즈 분포와 다분산 지수 (PI)를 확인하였으며, 샌드위치 효소 면역 측정법 (ELISA)를 이용하여 SARS-CoV-2 S 단백질과의 결합 여부를 확인하였다. 가장 고순도로 정제된 펩타이드 1을 사용하여 S 단백질에 대한 특이성 테스트를 진행하였으며 최종적으로 그래핀 전계효과 트랜지스터 (g-FET)에 고정하였다.

펩타이드 1이 고정된 g-FET는 전류-전압 곡선과 출력곡선을 통하여 g-FET 본래의 전기적인 성능을 유지하는 것을 확인하였다. 제작된 센서는 SARS-CoV-2의 S 단백질을 10 aM 검출한계 (LOD) 수준으로 감지하였으며 이는 매우 민감한 센서가 제작되었음을 제시한다. 또한 10^3 TU/mL의 농도를 갖는 SARS-CoV-2 유사 바이러스 (PV)를 검출하였다.

따라서 ACE2 유래 펩타이드는 SARS-CoV-2의 특이적이고 민감한 감지를 위한 나노바이오센서의 바이오 물질로 사용될 가능성이 있음을 제시한다.

Ⅲ iii

주요어: SARS-CoV-2, ACE2, ACE2-derived peptide, *E. coli,* Biosensor, Graphene-FET

학번: 2021-26535